PROCEEDINGS OF SCIENCE

Modelling very high-energy gamma rays detected from GRB 190829A: A comparative study

Monica Barnard,[a,*] **Soebur Razzaque**[a,b,c] **and Jagdish C. Joshi**[d,a]

[a] *Centre for Astro-Particle Physics (CAPP), Department of Physics, University of Johannesburg, PO Box 524, Auckland Park 2006, South Africa*

[b] *Department of Physics, The George Washington University, Washington, DC 20052, USA*

[c] *National Institute for Theoretical and Computational Sciences (NITheCS), South Africa*

[d] *Aryabhatta Research Institute of Observational Sciences (ARIES), Manora Peak, Nainital 263001, India*

E-mail: monicabarnard77@gmail.com, srazzaque@uj.ac.za, jagdishcjoshi86@gmail.com

Recent observations of very-high-energy (VHE, $\gtrsim$ 100 GeV) afterglow emission from a few gamma-ray bursts (GRBs) raised important questions regarding the emission mechanism responsible for this radiation. So far, synchrotron-self-Compton (SSC) has been primarily used to model VHE emission from GRBs. As a first approach we have applied NAIMA, a publicly available code for radiation modelling from relativistic electrons, to model GRB afterglow emission. We present predictions of multiwavelength energy spectra for GRB 190829A, assuming the emission is SSC in a wind scenario. In our prior work, using a code developed by us, the SSC model gave a satisfactory fit to the VHE data for a given set of fixed model parameters for this particular GRB, with a wind environment preferred over a constant density inter-stellar medium. NAIMA already includes optimisation tools to perform Markov Chain Monte Carlo (MCMC) fitting of radiative models to multiwavelength spectra. This is our motivation for this study of comparing optimised model parameters from NAIMA to those from our own code. Finding a more robust fit of the model to the observations has implications on future observations, especially by the CTA Observatory, implying better constraints on the GRB environment and the particle energy requirements for the emission observed at late times.

High Energy Astrophysics in Southern Africa 2023 (HEASA 2023)
September 5 - 9, 2023
Mtunzini, KwaZulu-Natal, South Africa

[*]Speaker

PoS(HEASA2023)017

1. Introduction

Gamma-ray bursts (GRBs) are characterised by short energetic bursts of radiation and are mainly divided into two categories based on duration, i.e., long (>2 s) and short (< 2 s), with the former GRBs originating mostly from the collapse of massive stars (see e.g., [1]). As the highly relativistic matter propagates into the surrounding environment it collects gas causing the resulting blastwave to slow down with time giving rise to the late-time afterglow emission of fading brightness.

The very-high energy (VHE; >100 GeV) afterglow emission from only a few GRBs have been observed by groundbased Cherenkov telescopes, including GRB 180720B [2], GRB 190114C [3], GRB 190829A [4], GRB 221009A [5], GRB 201015A [6] and GRB 201216C [7]. The VHE afterglow emission from GRB 190829A, with a redshift of z=0.0785 and a burst duration of T_{90}=63 s, was detected by *H.E.S.S.* above 3 TeV for the first night (T_0+4.3 hr), and above 1 TeV for the second night (T_0+27.2 hr) [4]. This same burst was observed for a third night but no significant emission was visible.

Several studies have attempted to explain the GRB afterglow emission in the sub-GeV to TeV band using synchrotron self-Compton (SSC; see e.g., [8–11]). Other studies assumed that the gamma-ray photons can be produced by the inverse Compton (IC) scattering of low energy seed photons by relativistic electrons accelerated at the blastwave, where the seed photons have an external origin (see [12, 13]). External Compton (EC) emission becomes relevant when the energy density of the external radiation field in the jet frame exceeds that of the energy density in the magnetic field. [12] explained the VHE emission using a combination of SSC and EC model, assuming both the wind and ISM environments, as well as the CMB as an external field, although the fit for GRB 190829A was dominated by SSC. [4] also explained the VHE emission from the latter GRB as SSC.

In this paper, we attempt to reproduce the results of [12] for GRB 190829A using a GRB emission modelling code known as NAIMA [15]. In Section 2 we describe the NAIMA emission model and present the application thereof in Section 3. We then compare our results to those found by [12], which include a fit to multiwavelength observations. Our conclusions follow in Section 4.

2. NAIMA emission model

The NAIMA emission model is an open source Python (Astropy affiliated) code that creates an interface between the radiation processes already coded in NAIMA (i.e., synchrotron, IC scattering, SSC, non-thermal Bremsstrahlung, and pion decay) and the physical parameters that would be needed to explain the multiwavelength emission of a GRB in a simple 1-zone SSC scenario. It is also used to analyse multiwavelength data of any other GRB afterglows (see [15] and references therein) and uses this framework to fit the data using a Markov-Chain Monte Carlo (MCMC) method. Basic expressions for GRB afterglows and the physical parameters used in this code to explain their emission, and to describe and explain the assumptions that are made can be divided into several categories:

- **Theoretical framework**: The relations derived in this code comes from the physics of the environment, and are in the shock frame. It computes the Lorentz factor of the forward shock,

Γ i.t.o. M the mass of the material swept by the shock and $E_{\rm iso}$ the isotropic energy ($\equiv E_{\rm k}$ the kinetic energy) of the GRB. There are two possible scenarios: a constant density of the interstellar medium surrounding the progenitor (ISM density profile resulted by a stellar wind - Wind Relativistic calculations give then the radius of the shock front, R, i.t.o. $\Gamma(R)$, and Δ_t the time since the explosion in the observer's frame. The number density of the target photon field, in NAIMA to compute the SSC component of the spectrum, we need to calculate the number of synchrotron photons produced in the emission zone, assuming that the emission comes from a thin shell. NAIMA does not perform time evolution, so the electrons injected have a broken power law distribution with an exponential cut-off at high energy.

- **Calculation of the minimum injection energy**: The minimum injection energy is a parameter that cannot be fixed a-priori, but depends on the fraction of energy that goes into the particles with respect to the total available energy at the shock [9, 12]. This parameter is usually called $\eta_{\rm e}$ ($\equiv \epsilon_{\rm e}$; the equivalent parameter that describes the amount of energy going into magnetic field is called $\eta_{\rm B}$, also $\equiv \epsilon_{\rm B}$). The ratio between the two branches of the exponential cutoff broken power law can be found analytically, but to avoid problems in the MCMC and to make the calculations stable, the ratios are computed numerically and the minimum energy is computed with an iterative procedure. Using the full electron distribution in the integrals, we first set the minimum energy to 1 GeV (as it is close to the rest mass energy of a proton) and then we compute how much the ratio between the first and the second term of the equation (calling it K) is away from 1. After this, we shift down the value of $E_{\rm min}$ by K. One iteration is enough to obtain a value $K \sim 1$ for a reasonable range of indices (most of the times within a factor 2 or less).

- **Calculation of the normalisation of the electron distribution**: Different particle distributions are contained in this code, i.e., exponential cutoff, broken power law, exponential cutoff broken power law, and log parabola. As we use $\eta_{\rm e}$ as a free parameter, we need to associate it with the actual normalisation of the electron distribution because this is the parameter that in the end NAIMA uses to build the electron distribution. It starts with the internal energy density of the shocked plasma. At this point we compute the $E_{\rm min}$ of the distribution from the values of α_1 ($\alpha_2 - 1$) and $\eta_{\rm e}$, and we construct an electron distribution with unitary normalisation. And then compute the integral to get the total energy density for this electron distribution, and assumed the volume is that of a spherical shell. The width of the shell is a numerical factor and depends on the environment assumed (ISM, wind or average). The average scenario is similar to an ISM scenario, but with parameters of the size of the shock that are an average of the wind and ISM cases. Then the normalisation parameter of the electron distribution is calculated.

- **Constrains from the age of the system**: The age of the system is given by the Lorentz-corrected time from the trigger and is where the time has been corrected for the relativistic boost (primed quantities are in the shock frame). This means that the cooling break should be in a position in the spectrum for which the energy of the particles have the same cooling time as the age of the system. For a generic GRB, using this relations can give some constrains on the intensity of the magnetic field imposing that the cooling time of the electrons at the break is at the same level as the age of the system. This constrain is implemented in the prior function and can be switched off in the initialisation (setting the cooling constrain option to False).

- **Calculation of the internal absorption**: The code takes into account the $\gamma\gamma$-absorption that affects the emitted high energy photons when they interact with the synchrotron photons inside the source (internal absorption). Thus, we need the number density of the target radiation field $n_{\rm ph}$ (already calculated) and the cross section of the absorption process (an analytical approximation). In this way we can compute the optical depth parameter τ. In the code there are two different implementations for the absorption: (1) the default one takes into account that in the same region we have both emission and absorption with the observed flux equal to the intrinsic flux times $1 - e^{-\tau}$ (see [16]), and (2) a simple implementation is the observed flux equal to the intrinsic flux times $e^{-\tau}$.

- **Physical parameters fitted to the data**: The final implementation puts together the inputs from the previous subsections to build the model using NAIMA. In the basic implementation, there are 5 parameters that are set free to vary: $\eta_{\rm e}$ the fraction of energy available as non-thermal electrons, $E_{\rm b}$ the energy of the break in the electron distribution, α_2 the power law index above the break in the electron distribution, $E_{\rm c}$ the cut-off energy of the electron distribution, and B the intensity of the magnetic field. With the exception of α_2, all parameters are fitted in logarithmic space (base 10). The low energy index α_2 is not a free parameter because we are using the assumption that the break in the electron distribution is a synchrotron cooling break so that $\alpha_1 = \alpha_2 - 1$ ($\equiv p$). The limits in which these parameters can vary are defined in the prior function. It is possible to add different model functions and different priors that are called in the implementation. As an example, the released code includes a different prior function in which the cut-off of the electron distribution is not limited by the equilibrium between acceleration and synchrotron cooling. The use of this prior can be initialised through the synchrotron no limit flag set to True.

The aim of using this multi-dimensional emission code is to model GRB afterglows.

3. Application of NAIMA to GRB afterglow emission

We applied the NAIMA code (see Section 2) to GRB 190829A and constructed multiwavelength SEDs for both nights. We explained the VHE emission as SSC in a wind environment (denoted by subscript w), assuming the electron distribution follows an exponential cutoff broken power law. In Table 1 we summarise the best-fit model parameter values obtained by NAIMA via the MCMC routine and the model fit parameters found by our code published in [12], for the same GRB and assumptions, and compare both studies.

In Figure 1 we found that an increase in the mass loss rate $\dot{M}$ leads to an increase in SSC, however this causes an increase in the density $n_{\rm w}$ as well. This is larger compared to [12] and also larger than typically assumed values in theoretical modelling. In the wind case NAIMA automatically calculates the density using the wind density equation. Also, an increase in $\alpha_2 = 3.5$ leads to a flatter curve for the synchrotron, although $p = 2.5$ (see Section 2) is within the typical

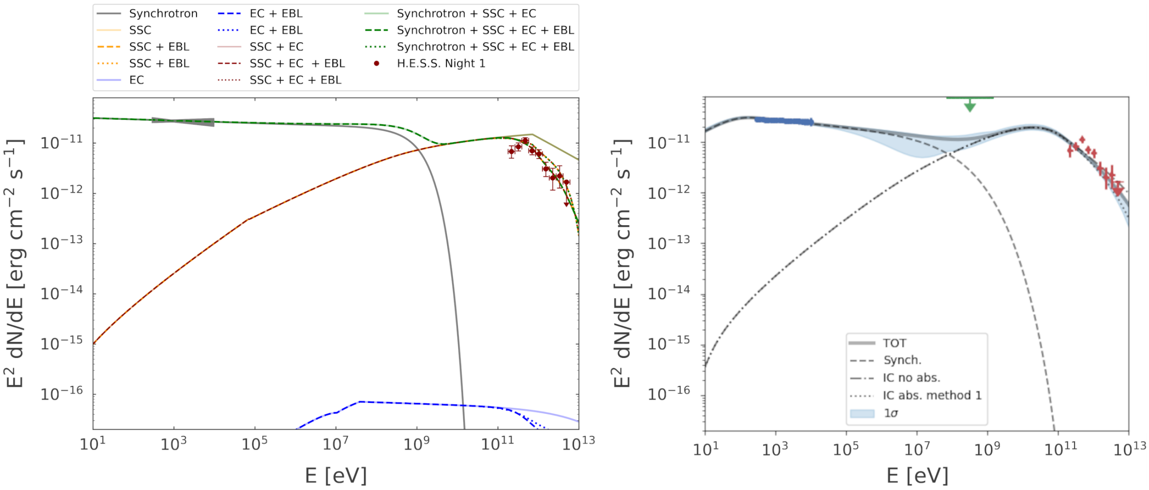

Figure 1: Multiwavelength SED for GRB 190829A for the first night. The left panel present results taken from [12], including the spectrum and uncertainty of the Swift-XRT data (shaded grey region, [4]) and the H.E.S.S. observations. The right panel is generated using NAIMA with the *Fermi* upper limit included.

range of values used for modelling. As ϵ_e is decreased, a shift of the SSC peak to higher energies is noticed, but not large enough and thus fitting the SSC spectral tail through the VHE data (see Figure (4) from [4]). The SSC peak becomes increasingly higher than the synchrotron if the tail is fitted. In Figure 2 we found similar behaviour as in Figure 1. Also, the Compton Y-parameter was taken as fixed ($Y = 1$ for EC to be relevant) by [12], whereas in theory $Y > 1$ for SSC emission to be important. The SED for both nights includes $\gamma\gamma$-absorption since without absorption the SSC spectrum would go up to a much higher energy than plotted. The internal absorption is negligible for GRB emission at late times with a value of $\tau < 1$ reported from NAIMA.

One should take note that there are discrepancies between the two comparisons such as that the NAIMA code does not include multiwavelength light curves which can be fitted simultaneously with the spectra, as done in [12]. There also exists a degeneracy in the parameter space used to fit the same GRB with the same assumptions, although the model fit parameters are not exactly the same and the resultant SED also differs. For instance the theory for the SSC radiation have been done numerically in NAIMA, whereas SSC is analytically calculated in [12] and could potentially cause this degeneracy. NAIMA computes Y from fitting the model to the data.

4. Conclusions

In our prior work, for a given set of fixed model parameters, we found that for GRB 190829A (both nights) the SSC gave a more satisfactory fit compared to the EC, when fitting the light curves and spectra simultaneously [12]. For this GRB the wind environment is preferred over constant density interstellar medium, with the Cosmic Microwave Background as the external radiation field. However, with the effective optimisation tool built in NAIMA we could find a more robust fit of the model to the data. However, with some discrepancies between NAIMA and our code [12], and even with an optimisation tool, one can not preclude better constraints on GRB physics of late-time VHE emission.

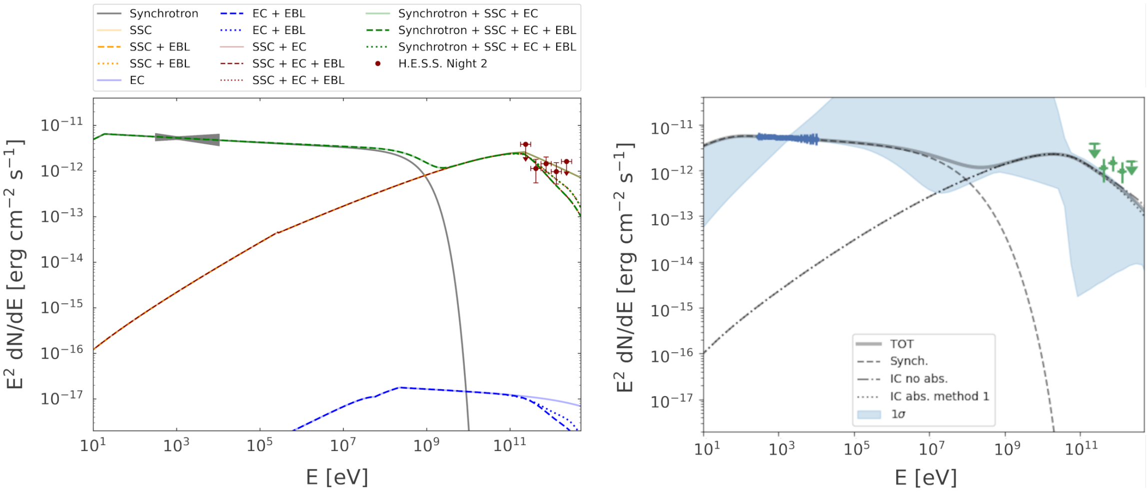

Figure 2: Same as Figure 1 but for the second night, and no *Fermi* upper limit.

Table 1: Summary of the afterglow parameter choices from fitting the multiwavelength spectra using NAIMA [15] and comparing it to our previous studies [12], assuming the wind environment in all cases.

Parameter	**GRB 190829A**			
	Night 1		**Night 2**	
	Barnard *et al.* (2024)	NAIMA	Barnard *et al.* (2024)	NAIMA
E_k (erg)	5.6×10^{51}	5.6×10^{51}	5×10^{51}	5×10^{51}
Γ_w	10	6	6	4
n_w (cm^{-3})	1.6×10^{-1}	5.8	2.8×10^{-2}	9.9
p	2.05	2.2	2.1	2.2
ϵ_e	9.1×10^{-2}	3.9×10^{-2}	9.1×10^{-2}	4.2×10^{-2}
ϵ_B	9.1×10^{-2}	2×10^{-3}	9.1×10^{-2}	3×10^{-3}
B' (G)	0.51	0.31	0.13	0.14
E_b (TeV)	0.005	0.027	0.019	0.047
E_c (TeV)	18.6	43.6	36.7	53.9
$Y = \sqrt{\epsilon_e/\epsilon_B}$	1	2.3	1	1.9

We need to include EC emission into the NAIMA code and use MCMC tool to find a more robust fit of the model to the observations to better constraint the emission. NAIMA must also be studied more and one needs to include multiwavelength light curves. Also, we can use our EC model and light curves as calibration in NAIMA and to rule out any degeneracy. In future we would apply model to more GRBs from which afterglow emission are observed at these extreme energies.

Acknowledgments

The research of MB was supported by a GES fellowship of University of Johannesburg (UJ), where this work was completed. SR acknowledges support from the National Research Foundation, South Africa for a BRICS STI grant, a grant from NITheCS and other grants from the UJ Research Council.

References

[1] S. E. Woosley, *Gamma-Ray Bursts from Stellar Mass Accretion Disks around Black Holes*, *ApJ*, **405**, 273 (1993).

[2] H. Abdalla *et al.*, *A very-high-energy component deep in the γ-ray burst afterglow*, *Nature*, **575**, 464 (2019).

[3] V. A. Acciari *et al.*, *Teraelectronvolt emission from the γ-ray burst GRB 190114C*, *Nature*, **575**, 455 (2019).

[4] H. Abdalla *et al.*, *Revealing x-ray and gamma ray temporal and spectral similarities in the GRB 190829A afterglow*, *Science*, **372**, 1081 (2021).

[5] Y. Huang, S. Hu, S. Chen, *et al.*, *LHAASO observed GRB 221009A with more than 5000 VHE photons up to around 18 TeV*, *GCN Circ.*, 32677 (2022).

[6] O. Blanch *et al.*, *MAGIC observations of GRB 201015A: hint of very high energy gamma-ray signal*, *GRB Coordinates Network*, **28659**, 1 (2020).

[7] O. Blanch *et al.*, *GRB 201216C: MAGIC detection in very high energy gamma rays*, *GRB Coordinates Network*, **29075**, 1 (2020).

[8] Xiang-Yu Wang *et al.*, *Synchrotron Self-Compton Emission from External Shocks as the Origin of the Sub-TeV Emission in GRB 180720B and GRB 190114C*, *ApJ*, **884**, 117 (2019).

[9] J. C. Joshi & S. Razzaque, *Modelling synchrotron and synchrotron self-Compton emission of gamma-ray burst afterglows from radio to very-high energies*, *MNRAS*, **505**, 1718 (2021).

[10] E. Derishev & T. Piran, *GRB Afterglow Parameters in the Era of TeV Observations: The Case of GRB 190114C*, *ApJ*, **923**, 135 (2021).

[11] M. Klinger, D. Tak, A. M. Taylor, & S. J. Zhu, *Probing the multiwavelength emission scenario of GRB 190114C*, **MNRAS**, **520**, 839 (2023).

[12] M. Barnard, S. Razzaque, & J. C. Joshi, *Very high energy gamma-rays from GRB 180720B and GRB 190829A with external Compton emission*, *MNRAS*, **527**, 11893 (2024).

[13] B. T. Zhang, K. Murase, P. Veres, & P. Mészáros, *External Inverse-Compton Emission from Low-luminosity Gamma-Ray Bursts: Application to GRB 190829A*, *ApJ*, **920**, 55 (2021).

[14] H. Zhang, I. M. Christie, M. Petropoulou, J. M. Rueda-Becerril, & D. Giannios, *Inverse Compton signatures of gamma-ray burst afterglows*, *MNRAS*, **496**, 974 (2020).

[15] V. Zabalza, *NAIMA: a Python package for inference of relativistic particle energy distributions from observed nonthermal spectra*, *Proceedings of International Cosmic Ray Conference 2015*, 922 (2015).

[16] G. B. Rybicki & A. P. Lightman, *Radiative processes in astrophysics* (1979).

[17] D. Foreman-Mackey, D. W. Hogg, D. Lang, & J. Goodman, *emcee: The MCMC Hammer*, *PASP*, **125**, 306 (2013).